Bulletin of the Seismological Society of America, Vol. 76, No. 6, pp. 1830–1837, December 1986



# THE NORTH PALM SPRINGS, CALIFORNIA, EARTHQUAKE SEQUENCE OF JULY 1986

BY LUCILE M. JONES, L. KATHERINE HUTTON, DOUGLAS D. GIVEN, AND CLARENCE R. ALLEN

An $M_L = 5.9$ earthquake occurred at 09:20 (UTC) on 8 July 1986 approximately 12 km northwest of the community of North Palm Springs, California. The epicenter of this earthquake was located between the Mission Creek and Banning strands of the San Andreas fault system at 34°0.0′N, 116°36.4′W. In this section of the San Andreas fault system, there is is a high level of diffuse microseismic activity, and it is not clear which of the many mapped fault traces is presently the most active strand (e.g., Allen, 1957; Matti *et al.*, 1985). The hypocentral distribution of the aftershocks as well as the focal mechanisms of the main shock and a few dozen aftershocks together suggest that the earthquake probably occurred on the Banning fault.

## ANALYSIS

*Seismotectonic setting.* The 1986 North Palm Springs earthquake occurred within the Central Transverse Ranges segment of the San Andreas fault (Figure 1; Matti *et al.*, 1985). There are several distinct strands of the fault system in this segment, and various nomenclatures have been used for these strands. We follow Matti *et al.* (1985) who based their scheme on the work of Allen (1957). The epicenter of the main shock was located between the Mission Creek strand of the San Andreas fault and the Banning fault, 25 km northwest of the point where these faults merge to form the Coachella Valley segment of the San Andreas fault. Both the Mission Creek and Banning faults show Recent movement and, at the longitude of the 1986 main shock epicenter, both faults dip 60° to 70° north at the surface (Allen, 1957). Presumably, the dips of both faults increase to near-vertical farther east, as they gradually bend southeastward to achieve a strike more parallel to that of the overall San Andreas system. Matti *et al.* (1985) divide the Banning fault into three segments. The epicenter of the 1986 main shock is located at the boundary of two of these segments, where the fault strike changes most abruptly from east to southeast. Just south of and subparallel to the Banning fault is the Garnet Hill fault, which breaks Quaternary alluvium at the mouth of Whitewater Canyon (Allen, 1957) and is mapped by Proctor (1968) and Matti *et al.* (1985) as extending more than 15 km to the southeast.

The largest previous earthquake in this area was the 1948 Desert Hot Springs earthquake ($M_L = 6.5$). Richter *et al.* (1958) associated this earthquake with the Mission Creek fault, in spite of the apparent lack of surface displacement. The offset of the epicenter from the surface trace of the Mission Creek fault has been ascribed either to a northward dip on the Mission Creek fault or to systematic location bias resulting from velocity contrasts across the fault. The 1948 earthquake was preceded by at least 13 yr of high levels of moderate earthquake activity. Ten events of $M_L \geqq 5.0$ were recorded between 1935 and 1948 in the region (Richter *et al.*, 1957). In contrast, only one $M_L \geqq 5.0$ event has occurred in the region between 1948 and 1986. The 1947 Morongo Valley ($M_L = 5.5$) earthquake was tentatively

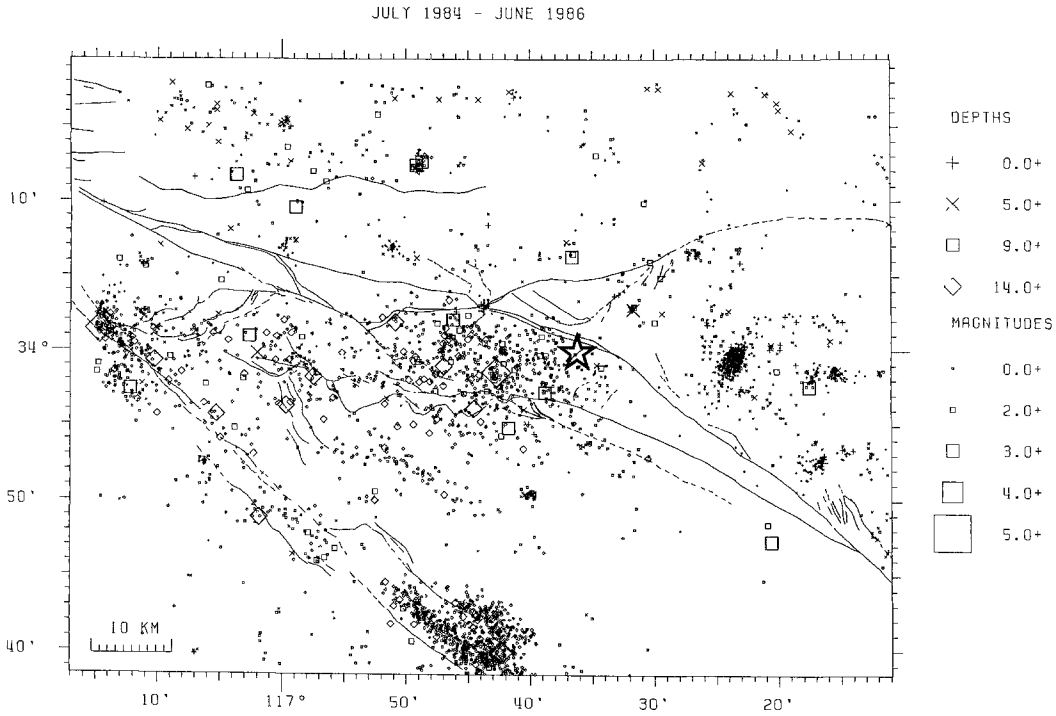


FIG. 1. A map of the North Palm Springs region showing the seismicity recorded by the southern California seismic network between July 1984 and June 1986. The location of the 8 July 1986 North Palm Springs earthquake ($M_L = 5.9$) is shown by a star. Fault traces are after Matti *et al.* (1985).

assigned to the Mission Creek fault by Richter *et al.* (1958), abutting the 1948 rupture zone. The 1944 Kitching Peak sequence ($M_L = 5.3$) could be associated with the Banning fault, on the section adjoining the 1986 rupture area.

Modern microseismic activity changes character near the epicenter of the 1986 main shock (Figure 1). To the west of the epicenter, a high level of seismic activity includes events with depths as great as 22 km concentrated between the Mission Creek and Banning faults (Green, 1983). East of the epicenter, the level of seismic activity is markedly lower, the events are shallower (usually less than 10 km depth), and almost all are located east of the Mission Creek fault.

*Data and techniques.* The main shock and aftershocks of the North Palm Springs sequence were recorded by the 238 stations of the Caltech-U.S. Geological Survey Cooperative Seismic Network in southern California. In addition, eight temporary analog seismic recorders were placed in the field on 9 and 10 July by the U.S. Geological Survey. Approximately 500 *P*-wave arrival times from these temporary stations have been added to the Caltech-U.S. Geological Survey data set. Three-hundred sixty-two of the aftershocks that were recorded between 8 and 31 July have been analyzed using the CUSP processing systtem (Johnson, 1983), including most of the $M_L \geqq 3.5$ events from that time. At this early stage of processing, only some of the recorded aftershocks have been timed and analyzed, although the larger aftershocks were preferentially selected for processing. Thus, no conclusions should be drawn from apparent temporal or magnitude distributions.

All of the phase data (*P*- and *S*-wave arrival times) come from the routine processing procedures. All of the earthquakes were relocated using HYPOINVERSE (Klein, 1985) and the velocity model in Table 1. This model was derived as part of a study of focal mechanisms on the San Andreas fault (Jones, 1985) and is based

on the results of Hadley and Kanamori (1978). Focal mechanisms for the North Palm Springs aftershocks were determined by the grid searching program FPFIT (Reasenberg and Oppenheimer, 1985) after correcting the polarities of reversed stations with the information of Norris *et al.* (1986). The first motions were picked during routine analysis and not rechecked; therefore, these results must be considered preliminary.

*Locations.* The $M_L = 5.9$ North Palm Springs main shock was located at 34°0.0N, 116°36.3'W at a depth of 11.3 km. The epicenters of the main shock and the aftershocks that have been processed to date are shown in Figure 2. In map view, the epicenters of the aftershocks form a rough ellipse 16 km long by 9 km wide striking northwest to west-northwest. The ellipse is symmetric around the epicenter of the main shock. Several of the largest aftershocks ($M > 4.0$) are located at the ends of the ellipse.

TABLE 1

VELOCITY MODEL

| *P*-Wave Velocity (km/sec) | Depth to Top of Layer (km) |
|---|---|
| 5.5 | 0.0 |
| 6.2 | 5.5 |
| 6.7 | 16.0 |
| 7.8 | 32.0 |

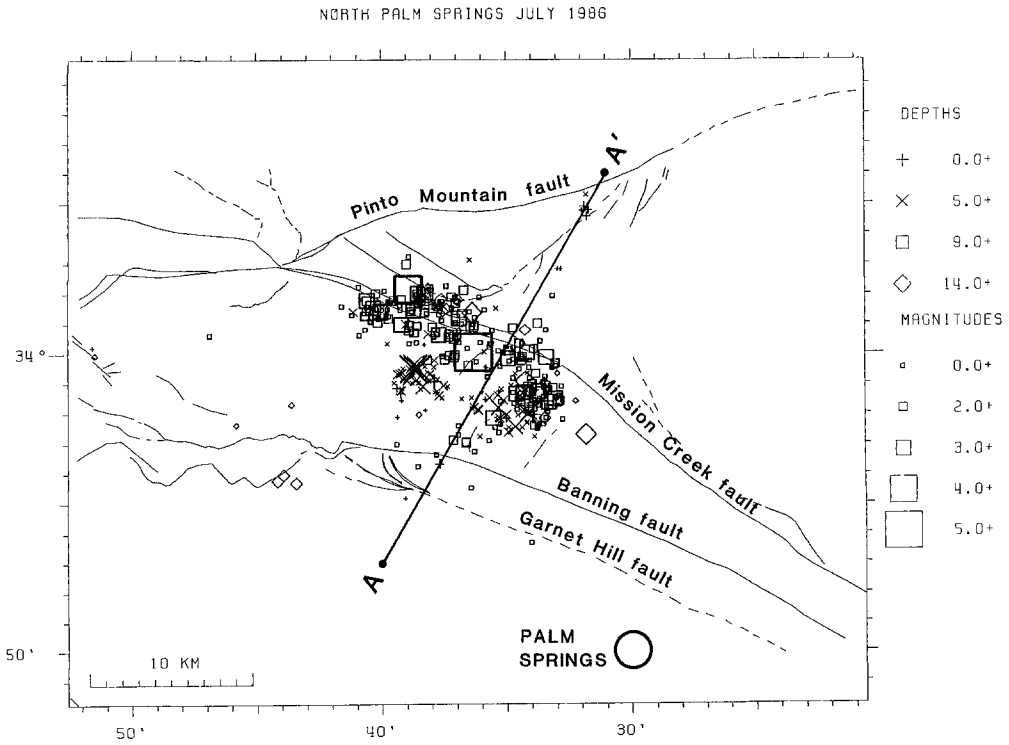


FIG. 2. The epicentral locations of the main shock and located aftershocks of the 8 July 1986 North Palm Springs earthquake ($M_L = 5.9$). The line *A-A* is the projection line for the cross-section in Figure 3. Fault traces are after Matti *et al.* (1985).

The calculated depths of the aftershocks are projected onto a plane trending N30°E in the cross-section of Figure 3. The western and eastern sections of the aftershock zone are plotted separately. Most of the aftershocks are located between 6 and 15 km depth. West of the main shock, the hypocenters cluster onto a plane that dips northeast at approximately 50°. At 11.3 km depth, the main shock is in the middle of the hypocentral distribution of the aftershocks. East of the main shock the hypocentral distribution is more diffuse. Preliminary results suggest that the rupture surface, as delineated by the aftershocks, may have a more southerly trend and may dip more steeply (60° to 70°) east of the main shock. However, a more detailed analysis than is possible here is needed to resolve this question. The largest aftershocks occur both at the shallowest and deepest extents of the aftershock distribution.

The distribution of the aftershocks suggests that the North Palm Springs earthquake ruptured on a surface trending approximately N60°W and dipping about 50° to the northeast. The central position of the main shock hypocenter within the hypocentral distribution indicates that the rupture during the main shock was bilateral or circular. The difference in the hypocentral distributions of the aftershocks to the east and west of the main shock suggests that the fault could change both strike and dip at the epicenter of the main shock.

*Focal mechanism.* The focal mechanism determined from first motions for the $M_L = 5.9$ main shock is shown in Figure 4. The preferred plane in the focal mechanism trends N60°W and dips north at 45°. The rake on this plane is 180° indicating pure right-lateral strike-slip motion. To test the stability of this solution, it was recomputed using several different velocity models to determine the takeoff angles. In all cases, the rake was 180° (pure right-lateral strike slip), the strike of the northwest-trending plane varied less than 10°, and the dip of that plane ranged from 43° to 50°.

The focal mechanisms determined for the analyzed $M \geqq 3.1$ aftershocks are shown in Figure 5. Most of the focal mechanisms determined for the aftershocks have one plane within 30° of the N60°W trending plane of the main shock solution, dipping

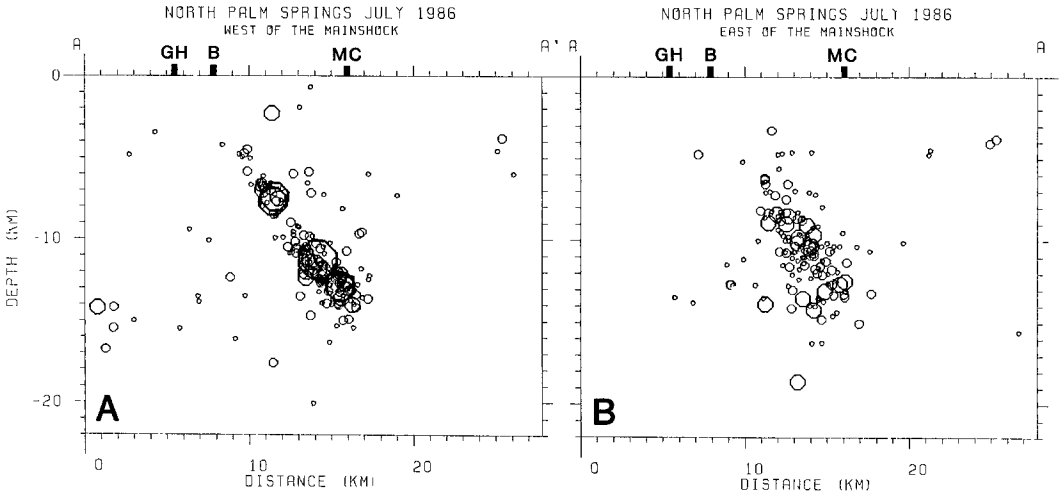


FIG. 3. The depths of the main shock and located aftershocks of the 8 July 1986 North Palm Springs earthquake ($M_L = 5.9$) plotted against their projection onto the line $A$-$A'$ shown in Figure 2. The points where the Garnet Hill (GH), Banning (B), and Mission Creek (MC) faults cross $A$-$A'$ are marked. Aftershocks west of the main shock (A) and east of the main shock (B) are shown separately.

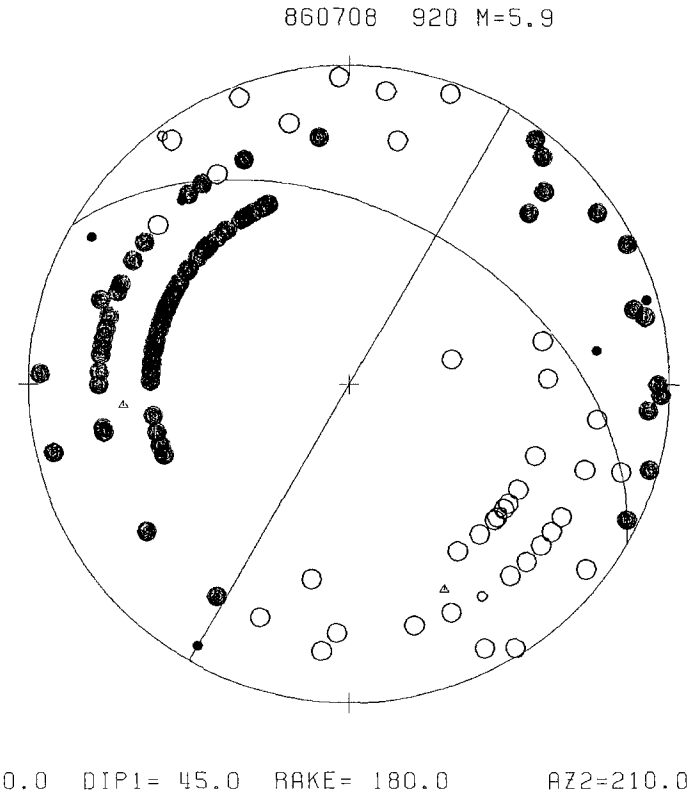


FIG. 4. The focal mechanism of the 8 July 1986 North Palm Springs earthquake ($M_L = 5.9$) determined with local first motions. Closed circles represent compressive first motions. Open circles represent dilatational first motions.

between 35° and 70°. The motion on this plane during the aftershocks ranges from pure right-lateral strike-slip as seen in the main shock through oblique right-lateral reverse to almost pure reverse motion. No dependence of the type of focal mechanisms on depth could be seen. Reverse motion is evident in both shallow and deep aftershocks.

## DISCUSSION

The North Palm Springs earthquake ruptured a fault trending N60°W and dipping north at 45° to 55°. The first motions of the main shock show right-lateral strike-slip motion on this plane. Focal mechanisms of many of the aftershocks also show a component of oblique reverse motion with the right-lateral strike slip. The focal mechanisms of the aftershocks are similar to single event focal mechanisms determined for small independent earthquakes that occurred in this region during the last decade (Green, 1983; Jones, 1985; Webb and Kanamori, 1985). Although the first motions of the main shock show only strike-slip motion, this is not incompatible with the observation of some reverse component to the motion in teleseismic solutions reported by J. Nabelek (personal communication, 1986). The earthquake could have begun with horizontal motion resulting in the strike-slip local focal mechanism shown here and then developed a vertical component later in the rupture producing a reverse component in the longer period teleseismic solutions.

A recent study of this region by Nicholson *et al.* (1986) has proposed that much

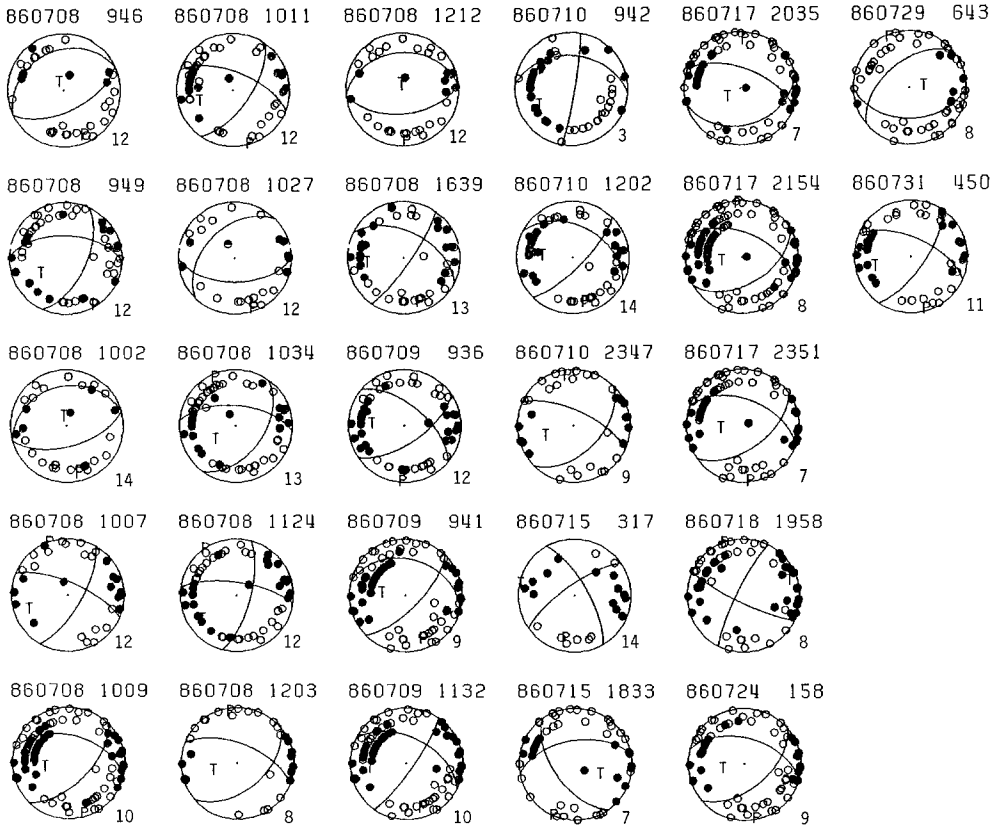


FIG. 5. Focal mechanisms of $M \geq 3.1$ aftershocks of the 8 July 1986 North Palm Springs earthquake from local first motions determined by FPFIT. Symbols are as in Figure 4. The depth in kilometers of each aftershock is shown in the *right* of its focal mechanism.

of the modern seismicity results from slip on northeast-trending faults, but it is obvious that the North Palm Springs earthquake occurred on a northwest-trending fault. Nicholson *et al.* (1986) also proposed a decollement surface at 10 to 12 km depth based on variations in the type of faulting seen in composite focal mechanisms. No change in the type of focal mechanism with depth is evident in the aftershocks of this earthquake. There is a gap in the hypocentral distribution west of the main shock at 8 to 9 km depth, but very preliminary locations not included in this letter suggests that this results from the incompleteness of data processing.

From the cross section of Figure 3, taken together with the focal mechanisms, it would be reasonable to project the rupture plane to the ground surface alone either the Banning or the Garnet Hill fault. We think that the Banning fault is the most likely causative structure for this earthquake, in view of the fault's known northerly dip, its demonstrated ongoing creep (Louie *et al.*, 1985), and its regional tectonic importance. On the other hand, in the absence of clear evidence of surficial tectonic displacement during this earthquake (Sharp *et al.*, 1986), it cannot be stated with complete confidence that the earthquake was necessarily related to slip on any mapped fault.

It should be noted that the aftershock zone of the earthquake strikes northwest along its entire 16 km length. The westernmost part of the aftershock zone extends beyond the mapped trace of the Garnet Hill fault but does not change strike to a more easterly orientation as does the Banning fault. This lack of agreement between

the strike of the aftershock zone and the strikes of mapped faults should be viewed in light of the 6 to 15 km depth range of aftershock hypocenters. It could be that the fault structures at depth are quite different from the surface geology of this region as observed in regions of thrust faulting.

In conclusion, the North Palm Springs earthquake has provided insight into the mechanics of an area of extremely complicated fault geometry. First, it has shown again that strands of the San Andreas fault system can produce moderate earthquakes, so that great earthquakes are not the only possible strain release mechanism in this region. Second, these results demonstrate that strike-slip motion can occur on shallowly dipping faults. It also suggests that the Banning fault does not steepen with depth as previously proposed but rather maintains a dip close to 50° to a depth of at least 15 km. Third, the lack of correlation between trends of the surface faults and the aftershock zones demonstrates the inadvisability of presuming that there must be a direct correlation between surficial geologic features and seismogenic structures at depth.

## ACKNOWLEDGMENTS

Analysis of this earthquake would have been impossible without the hard work and dedication of the Caltech and U.S. Geological Survey seismic data analysts, Riley Geary, Kathy Watts, Steven Bryant, Robert Norris, and Ruth Hannah. The temporary analog seismic stations were operated in the field by Rob Wesson, Craig Nicholson, John Coakley, and Gonzalo Mendoza of the U.S. Geological Survey. The *P*-wave arrival times from the temporary stations were supplied by Rob Wesson, Rex Allen, and Craig Nicholson. Egill Hauksson and Susanna Gross of the University of Southern California helped in the preparation of data for analysis. Tom Heaton, Steve Hartzell, and Egill Hauksson supplied critical reviews. Caltech's contributions to this study were funded in part by U.S. Geological Survey Cooperative Agreement No. 14-08-0001-A0257.

## REFERENCES

Allen, C. R. (1957). San Andreas fault zone in in San Gorgonio Pass, southern California, *Bull. Geol. Soc. Am.* **68,** 315–350.

Green, S. M. (1983). Seismotectonic study of the San Andreas, Mission Creek, and Banning fault systems, *M.S. Thesis*, University of California at Los Angeles, Los Angeles, California, 52 pp.

Hadley, D. and H. Kanamori (1978). Seismic structure of the Transverse Ranges, California, *Bull. Geol. Soc. Am.* **88,** 1469–1478.

Johnson, C. E. (1983). CUSP—Automated processing and management for large, regional seismic networks (abstract), *Earthquake Notes* **54,** 13.

Jones, L. M. (1985). Focal mechanisms and state of stress on the San Andreas fault in southern California, *Trans. Am. Geophys. Union* **66,** 953.

Klein, F. W. (1985). User's Guide to HYPOINVERSE, a program for VAX and PC350 computers to solve for earthquake locations, *U.S. Geol. Surv., Open-File Rept. 85-515*, 24 pp.

Louie, J. N., C. R. Allen, D. C. Johnson, P. C. Haase, and S. N. Cohn (1985). Fault slip in southern California, *Bull. Seism. Soc. Am.* **75,** 811–833.

Matti, J. C., D. M. Morton, and B. F. Cox (1985). Distribution and geologic relations of fault systems in the vicinity of the Central Transverse Ranges, southern California, *U.S. Geol. Surv., Open-File Rept. 85-365*, 23 pp.

Nicholson, C., L. Seeber, P. Williams, and L. R. Sykes (1986). Seismicity and fault kinematics through the Eastern Transverse Ranges, California: block rotation, strike-slip faulting and low angle thrusts, *J. Geophys. Res.* **91,** 4891–4908.

Norris, R., C. E. Johnson, L. M. Jones, and L. K. Hutton (1986). The Southern California Network Bulletin, *U.S. Geol. Surv., Open-File Rept. 86-96*, 31 pp.

Proctor, R. J. (1968). Geology of the Desert Hot Springs-Upper Coachella Valley area, California, *California Division of Mines and Geology Special Report 94*, 50.

Reasenberg, P. and D. Oppenheimer (1985). FPFIT, FPPLOT and FPPAGE: Fortran computer programs for calculating and displaying earthquake fault-plane solutions, *U.S. Geol. Surv., Open-File Rept. 85-739*, 46 pp.

Richter, C. F., C. R. Allen, and J. M. Nordquist (1958). The Desert Hot Springs earthquakes and their tectonic environment, *Bull. Seism. Soc. Am.* **48,** 315–337.

Sharp, R. V., M. J. Rymer, and D. M. Morton (1986). Trace-fractures on the Banning fault created in in association with the 1986 North Palm Springs earthquake, *Bull. Seism. Soc. Am.* **76,** 1838–1843.

Webb, T. H. and H. Kanamori (1985). Earthquake focal mechanisms in the eastern Transverse Ranges and San Emigdio Mountains, southern California, and evidence for regional decollement, *Bull. Seism. Soc. Am.* **75,** 737–757.

U.S. GEOLOGICAL SURVEY
SEISMOLOGICAL LABORATORY
CALIFORNIA INSTITUTE OF
TECHNOLOGY, 252-21
PASADENA, CALIFORNIA 91125
(L.M.J., D.D.G.)

SEISMOLOGICAL LABORATORY
CALIFORNIA INSTITUTE OF
TECHNOLOGY, 252-21
PASADENA, CALIFORNIA 91125
CIT CONTRIBUTION NO. 4394
(L.K.H., C.R.A.)